

8. Multifractal Analysis of the Badland Formation

8.1 Introduction

There is a lack of understanding regarding certain issues of badlands in particular, which cannot be fully addressed by the drainage morphometric analysis method. The drainage morphometric approach falls short of revealing the implicate complexity of badlands patterns over space and time. Limitations of drainage morphometry are primarily due to the scale of the base map from which the drainage map has been extracted and secondly, it does not consider the dynamic nature of the rill-gully-channel network. Furthermore, the morphometric approach has inherent limitations of the parameters used in the analysis. Drainage density, drainage frequency, drainagetexture, ruggedness number, etc, hold good for drainage systems, but in the case of badlands, these parameters do not quantify the intricacies of badlands forms. Badlands differ from a common drainage system in the sense that they spread through headward erosion more dominantly. Headward erosion develops rills-gullies at finer levels of observation which cannot be addressed through morphometric analysis as it considers streams only and not the gullies and rills. If lengths and numbers of gullies and rills are to be essentially considered, there would be no limit to drainage density and drainage frequency when the scale is continuously magnified at higher degrees (Ariza-Villaverde et al., 2013). Real et al. (2020) and Cao et al. (2020) have only recently applied multifractal analysis on the problems of gully erosion, making important correlations of the parameters.

Badlands show spatio-temporally patterns of gully-channel networks and are not in equilibrium with the runoff of the land (Guzman et al., 2018; Sidle et al., 2019; Liu et al., 2021). Therefore, a pattern-based analytical approach is required to deal with the problem of badlands. The present work attempts at advancing interpretation of multifractal method in regard to the badlands. The application of multifractal analysis in this work has provided significant insight into patterns and behaviour of badlands by characteristic quantification of the complexity of the gully network organization. This work shows that multifractal analysis may prove to be an essential approach for management and planning in areas affected by active gullies.

Very few researches are available, particularly on the application of multifractal analysis on the gully erosion and therefore more researches are required to develop an understanding of various aspects of the pattern, processes and planning of the badlands systems. Thus, the main objectives of this chapter are to (a) develop geomorphological correlation and interpretation of multifractal analysis for badlands patterns and (b) develop an understanding of badlands processes in space and time.

8.2 Methodology

The toposheet which is available for the study area was surveyed around 1987 - 88 on the scale of 1: 50,000. At this scale the detailed study of such dynamic features like gully will be compromised. For this purpose, the extraction of gully shoulder and ephemeral drainage lines can only be feasible through high resolution DEM (Digital Elevation Model) and high-resolution satellite images. Unfortunately, DEM of such desirable quality is not freely available. In the search of high-resolution free satellite images, Google Earth Pro provides

high resolution images at a scale of 1:20,000. From these images gully shoulders or boundaries are delineated in a GIS environment at the maximum resolution provided by Google Earth Pro (4800 × 4800 pixels). For this analysis we have use Esri ArcGIS (10.6). Moreover, the oldest high-quality image in Google Earth Pro in this area is available from 2003. For the detection of considerable change in landscape, image of two time intervals (2003 and 2018) in a gap of fifteen years are chosen For multifractal analysis, we have chosen four un-intervened or minutely intervened gully sites, so that the legitimacy of the analysis remains constant (Figure 8.1).

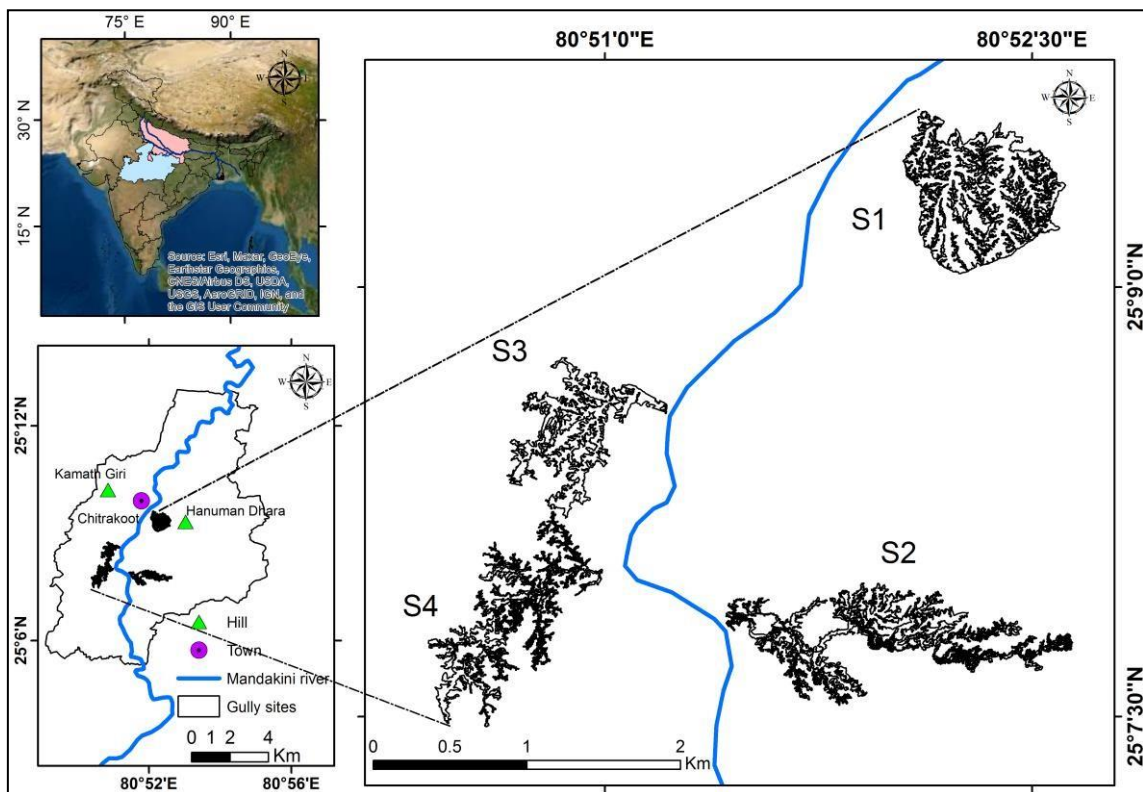


Figure 8. 1 Map of the study area showing the gully sites S1, S2, S3 and S4

The multifractal and lacunarity analysis were carried out in NIH's (National Institutes

ofHealth of United State) ImageJ software (version 1.53e) with binary images. Several different sites have been studied individually, so ROI (Region of Interest) was taken, in accordance to different scales and area of the images.

In order to correlate the patterns of the badlands with the climate, 50 years rainfall data (IMD) was used for the determination of Standard Precipitation Index (SPI). The detailed methodology adopted for the calculation of SPI is mentioned in Appendix-B.

8.2.1 Description of the Multifractal Parameters

Various parameters used in the multifractal analysis are defined below:

Fractal form: The essential characteristic of fractal patterns, which may be spatial and/or temporal in nature, is the iteration of self-similar forms at varying scales of observation. This complexity divulges that a pattern consisting of a one-dimensional element not only fills the space quantitatively but qualitatively as well, such that at any scale of observation, the pattern is observed to be present (Mandelbrot, 1982).

Fractal dimension: In fractal geometry, a fractal dimension is a ratio providing a statistical index of complexity comparing how details in a fractal pattern change or keep on maintaining with the change of scale at which it is measured. This characteristic non-integer dimension of self-similar fractal form is called fractal dimension and it remains scale-invariant. It has been therefore characterized as a measure of the space-filling capacity of a pattern that tells how a fractal scales differently from the space in which it is embedded (Mandelbrot 1982; Falconer et al., 2004; Vicsek, 1992).

Generalized dimension (D_q) and exponent Q : In the multifractal analysis, the generalized dimension, D_q , addresses how mass varies with ε (resolution or box size) in an image. It

shows the distortion of the mean (μ) of the probability distribution for pixels at some ε . D_q is used to generate multifractal spectra.

Q is an arbitrary exponent related to the distortion of a dataset. Q is part of generalised dimension D_q , which is a key variable in multifractal analysis.

D_q versus Q : In a multifractal pattern, this correlation gives a sigmoidal graph. The intersection of the sigmoidal curve with $q=0$ line gives the value of the fractal dimension. The typical sigmoidal form of the curve decreasing towards a higher degree of distortion ($q>0$; D_q values decreasing towards higher values of q) confirms the multifractal nature of the pattern.

α and $\Delta\alpha$: The α is an exponent of size, also called Holder's exponent (Feder, 1988) and is related to the probability of a number of pixels 'm' appearing in the i^{th} box. The difference $(\alpha)_{\text{max}} - (\alpha)_{\text{min}}$ of the graph on the range of α is $\Delta\alpha$. The greater the difference, the more complex is the multifractal pattern.

$f(\alpha)$ and $\Delta f(\alpha)$: The $f(\alpha)$ is called multifractal function of the components, which is a function of α , as it describes the local degree of singularity or regularity around the point α . The $\Delta f(\alpha)$ is a significant parameter of difference between the values of $f(\alpha)$ for the $(\alpha)_{\text{max}}$ and $(\alpha)_{\text{min}}$.

$f(\alpha)$ versus α : The $f(\alpha)$ versus α graph gives significant information of the distribution of fractal dimension of a subset of data, where exponent α is taken on the horizontal axis showing the range of scale and the parameter $f(\alpha)$ is taken on the vertical axis showing dimensions of subsets of the dataset.

The equations applied in the multifractal analysis used in the software ‘Image J’ are given below (Chhabra and Jensen, 1989):

$$Dq = \lim_{\varepsilon \rightarrow 0} \left[\frac{\ln I_{[Q, \varepsilon]} / \ln \varepsilon^{-1}}{(1 - Q)} \right] \quad (8.1)$$

$$I_{[Q, \varepsilon]} = \sum_{i=1}^N [P_{(i, \varepsilon)}]^Q \quad (8.2)$$

For $Q=1$, let $\varepsilon \rightarrow 1$ and $Dq = - \lim_{\varepsilon \rightarrow 1} \left[\frac{\sum_{i=1}^N P_i \ln [P_i] / \ln \varepsilon}{(1 - 1)} \right]$
(8.3)

The probability distribution is found from the number of pixels, M that was contained in eachⁱth element of a size= ε required to cover an object:

$$P_{(i, \varepsilon)} = \frac{M_{(i, \varepsilon)}}{\sum_{i=1}^N M_{(i, \varepsilon)}} \quad (8.4)$$

Thus, $P(i)$ is found from the probability distribution of mass or all boxes i , at this ε

Where $\sum_{i=1}^N P_{(i, \varepsilon)}^{Q=1} = 1$ and $\sum_{i=1}^N P_{(i, \varepsilon)}^{Q=0} = N_\varepsilon$ the number of boxes containing pixels

$$P_{(i, \varepsilon)} = \frac{\text{pixels}_{(i, \varepsilon)}}{\sum_{i=1}^N \text{pixels}_{(i, \varepsilon)}} \quad (8.5)$$

According to the method of Chhabra and Jensen (1989):

$$\mu(I_{[Q, \varepsilon]}) = P_i^Q \left/ \sum_{i=1}^N P_i^Q \right. \quad (8.6)$$

$$\alpha[Q, \varepsilon] = \left[\sum_{i=1}^N (\mu(I_{[Q,\varepsilon]}) \times \ln P_{(i)}) \right] / \ln \varepsilon \quad (8.7)$$

$$f(Q) = \left[\sum_{i=1}^N (\mu(I_{[Q,\varepsilon]}) \times \ln \mu(I_{[Q,\varepsilon]})) \right] / \ln \varepsilon \quad (8.8)$$

$$\tau_{(Q)} = (Q - 1) \times Dq \quad (8.9)$$

$$\text{And } f_{(\alpha[Q,\varepsilon])} = Q \times \alpha(Q) - \tau(Q) \quad (8.10)$$

8.2.2 Description of the Lacunarity

The word lacunarity means lack or gap (Mandelbrot, 1982). In the field of morphology, inhomogeneity, gappiness, visual texture, translational and rotational invariance etc, may be used to distinguish spatial patterns through the analysis of gap distribution in different scales (Plotnick et al., 1996; Khorasani et al., 2011; Charadram et al., 2012; Real et al. 2020). The sliding box method was used for Lacunarity analysis in ImageJ software. Then, average lacunarity (Λ) or λ for each grid g i.e. λ_g or Λ_g is

$$\Lambda_g = \left[\sum_{g=1}^{Box\ sizes} \lambda_{\varepsilon, \lambda_{\varepsilon, g}, g} \right] \div Box\ Sizes \quad (8.11)$$

$$\lambda_{\varepsilon, g} = (\sigma/\mu)_{\varepsilon, g}^2 \quad (8.12)$$

where λ is each lacunarity value; ε is the size of pixels; σ denotes standard deviation; μ signifies mean the number of pixels per box (Karperien, 2007- 2012).

A high lacunarity value explains a larger degree of gaps in the image. It also helps to understand the formational structure of the system by measuring the degree of inhomogeneity (Mandelbrot, 1982).

8.3 Results

8.3.1 Multifractal Analysis of the Badlands Sites

The present study includes interpretation of D_q versus q , $f(\alpha)$ versus α , $\Delta f(\alpha)$ and $(\Delta\alpha)$ in terms of patterns and geomorphic processes for the four sites, S1, S2, S3 and S4 of the Mandakini River watershed of Chitrakoot and it examines changes in the parameters of fractal analysis spatially and temporally.

D_q versus q : The importance of the range of D_q on the various degree of q provides an insight into the dimension of the fractal pattern. The higher the dimension, the more complex is the behavior of the fractal forms of badlands pattern. The plots have been used to understand the fractal nature of the gully channel erosive systems operative in the area.

The fractal dimensions of the badlands site S1 in the year 2003 and for the sites S2, S3, S4 in the year 2006 are 1.77, 1.59, 1.67 and 1.68, respectively. The S2 site has a minimum value of the fractal dimension of the order of 1.59, whereas the S1 site has the maximum order of 1.77. Similarly, the fractal dimensions of the badlands sites S1, S2, S3, S4 for the year 2013 are 1.76, 1.61, 1.62 and 1.65, respectively, whereas, for the year 2018, the values are 1.78, 1.63, 1.64 and 1.63 respectively (Table 8.1) (Figure 8.2 and 8.3).

Table 8. 1 Multifractal parameters of the multifractal spectra and lacunarity values of the gullysites S1, S2, S3, S4

Gully Site	Year	Dq	Δg	α_{\max}	α_{\min}	$\Delta\alpha$	$f(\alpha_{\max})$	$f(\alpha_{\min})$	$\Delta f(\alpha)$
S1	2003	1.77	0.2801	2.499	1.655	0.844	0.604	1.155	-0.551
	2013	1.76	0.2842	2.343	1.618	0.725	0.875	1.096	-0.221
	2018	1.78	0.2766	2.477	1.619	0.858	0.618	1.078	-0.460
S2	2006	1.59	0.393	2.436	1.405	1.031	0.688	0.934	-0.246
	2013	1.61	0.311	2.420	1.405	1.014	0.569	0.781	-0.212
	2018	1.63	0.295	2.540	1.354	1.186	0.546	0.742	-0.196
S3	2006	1.67	0.372	2.340	1.529	0.812	0.703	0.920	-0.216
	2013	1.62	0.460	2.267	1.458	0.810	0.590	0.785	-0.195
	2018	1.64	0.451	2.228	1.529	0.699	0.706	0.953	-0.246
S4	2006	1.68	0.401	2.383	1.570	0.813	0.583	1.103	-0.520
	2013	1.65	0.379	2.478	1.542	0.935	0.574	1.113	-0.539
	2018	1.63	0.477	2.343	1.495	0.85	0.687	1.019	-0.332

$f(\alpha)$ versus α :

Graphs of $f(\alpha)$ versus α from table 8.1 show variations in fractal parameters over the four sites for the years 2003/2006, 2013 and 2018 (Figure 8.2 and 8.3). These graphs for the study area are hump-shaped, right-skewed in nature with the following values:

The value of $(\Delta\alpha)$, i.e. $(\alpha)_{\max} - (\alpha)_{\min}$ of the graph on the range of α for the site S1 in 2003 is 0.691 and for the sites, S2, S3, S4 in the year 2006 is 1.031, 0.812 and 0.813 respectively. Similarly, the difference of $f(\alpha)$ for $(\alpha)_{\max}$ and $(\alpha)_{\min}$ denoted as $\Delta f(\alpha)$ is -0.587 for S1 and -0.246 (2003), -0.216 and -0.520 in 2006 for the site S2, S3, S4, respectively (Table 8.1) (Figure 8.2 and 8.3).

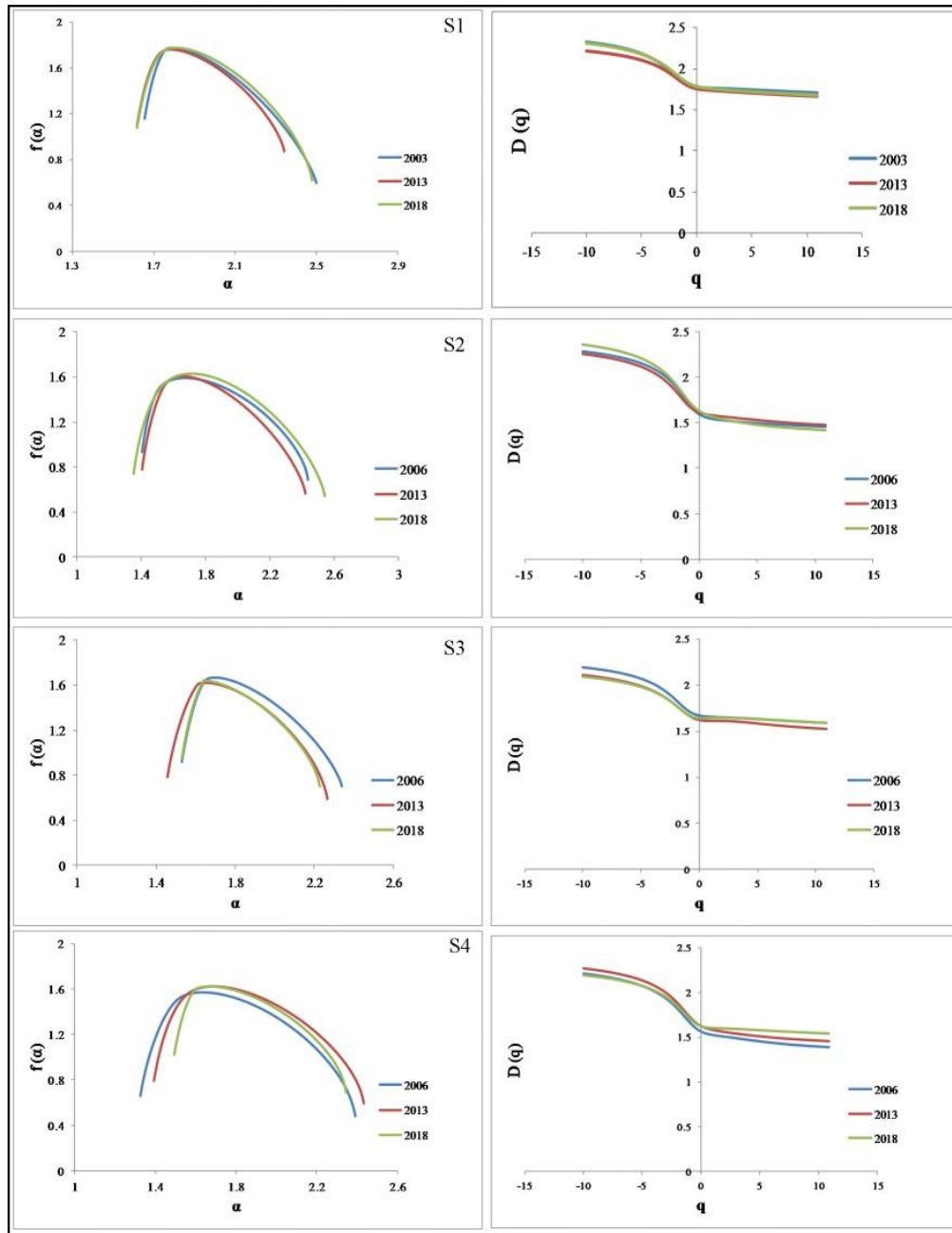


Figure 8. 2 Multifractal and fractal spectral curve of gully site S1, S2, S3, and S4

For the year 2013, $\Delta\alpha$ value for the range of scale is 0.744, 1.014, 0.810 and 0.935 and the value of $\Delta f(\alpha)$ is -0.725 for S1 and -0.212, -0.195 and -0.539 for the site S1, S2, S3, S4 respectively. In the year 2018, the values of $\Delta\alpha$ are 0.482, 0.546, 0.706, 0.690 and the values

of $\Delta f(\alpha)$ are -0.741, -0.196, -0.246, -0.085 for the sites S1, S2, S3, S4 respectively (Table 8.1) (Figure 8.2 and 8.3).

8.3.2 Lacunarity Analysis of the Badlands Sites

The lacunarity analysis is imperative in the multifractal analysis. Lacunarity can be defined as a complementary measure of fractal dimension or the deviation of a geometric structure from its translational invariance (Gefen et al., 1984). When fractal dimension (D_q) and $\Delta f(\alpha)$ provide idea about the multifractal nature of patterns of a form and confirm the complexity of space occupancy of the pattern, the lacunarity analysis further assures the multifractal nature of the pattern and provides insight into gappiness or in other words tightness of the patterns. Also, it gives an idea about the homogeneity or heterogeneity of a pattern. The lacunarity values of all the sites under consideration (Table 8.1 and Figure 8.1) are very low, which are less than one.

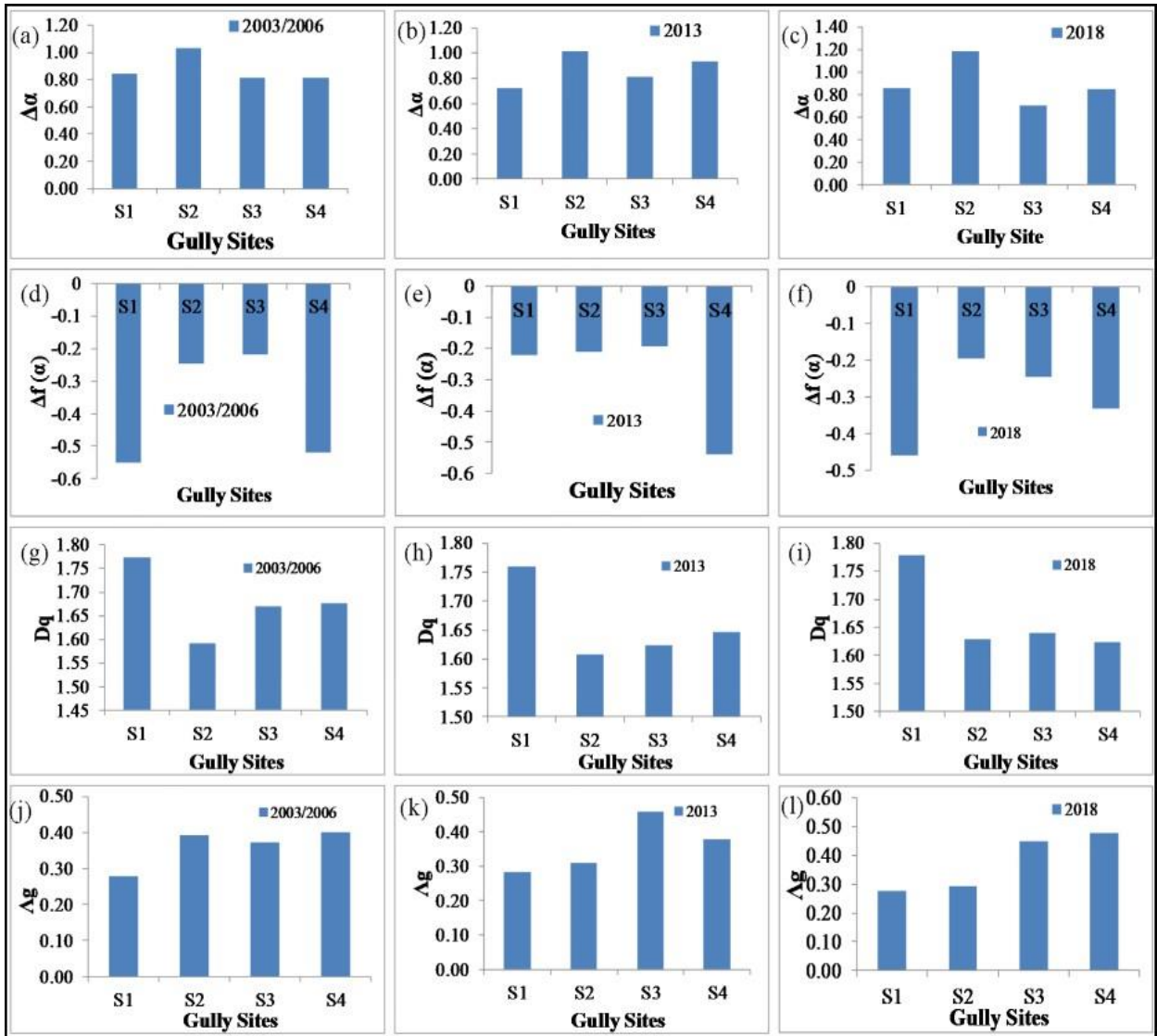


Figure 8. 3 Histogram of $\Delta\alpha$ (a-c), $\Delta f(\alpha)$ (d-f), Dq (g-i) and Λ_g (j-l)

8.4 Discussions

The multifractal asymmetry is related to fractal dimension distribution on various scales of observations as earlier researchers have found that natural phenomena are usually asymmetric multifractals (Szczepaniak and Macek, 2008; Drozd and Oswiecimka, 2015) instead of concave symmetric ones. The heterogeneity and entropy of the system may be explained by the degree of asymmetry (Posadas et al., 2005). Nonetheless, the right-side

asymmetry is still not fully explained and correlated with the processes of natural systems (Drozd and Oswiecimka, 2015). The problem of soil erosion has been addressed by Luo et al. (2018) with multifractal approach. Cao et al. (2020) worked on the identification of the active gully erosion sites on the loess of China using multifractal analysis. Real et al. (2020) made a significant contribution to the proposition of a new classification of gully erosion using multifractal and lacunarity analysis of a watershed in Brazil.

Multifractal analysis proves that the land has been dissected by gullies with more than one type of pattern of gully links, i.e., branching organization. The analysis shows that the dissection of lands is not random or without any organization pattern but has forms that have singularities indicating identical arrangements of a certain type of occurrences of forms—the fractal forms.

D_q versus Q : The curves for study sites of badlands are sigmoidal in nature, confirming that these badlands sites comprise multifractal patterns having fractal dimensions ($D_q=0$) between 1.6 to 1.78. These results prove that the badlands are quite complex in their organisation with multiple self-similar forms of gully networking systems (Real, 2020).

In the absence of any other natural causes, human interference, especially for conservative measures for the reclamation of lands, can also be deciphered from changes in the values of fractal dimensions over time. Drozd and Oswiecimka (2015) found that small-scale event fluctuations could interfere with the entire multifractal object of study. The four sites show interesting histories over the last fifteen years. The sites S1 and S3 have identical trends and history that their fractal dimensions were high in 2003 and 2006 respectively but declined by the year 2013 due to conservation measures by the villages for partial

reclamation of lands. Nevertheless, the fractal dimensions of the two sites again show a rising trend in 2018. The S1 site again turns out to be the most severely affected site approaching the value of the order of 1.78. Site S2 has a continuous trend of increase in fractal dimension through the same observation years. This site has not been reworked by conservation measures. The values of fractal dimensions are sensitive and were found to change under natural conditions through time to higher values indicating that the patterns grow in complexity and are self-enhancing in nature. This finding expresses that after initiation of gullying, the complexity of organization goes on increasing with branching of gully links towards upstream lands. It is notable that the rate of increase in fractal dimension is extremely slow and this shows the natural controlling impact of the indigenous bush cover over the soils in this site. Such upstream spreading of gullies makes headway by further deteriorating the physico-chemical properties of the soils. Site S4 has a continuously declining trend of fractal dimension and has been continuously controlled by soil conservation practices.

The multifractal dimension values show an increase in fractal dimension for S1 and S3 sites of the area in the year 2018 after a decline in 2013. This has a significant implication regarding the material used in conservative measures and shows that the badlands processes continue to regenerate their old pattern into the filled gullies. The regeneration of gullies on the filled gullies in such a short span of five years suggests that the gullies were filled with the same deteriorated earth material of the badlands. Any reclamation measures reduce the fractal dimension value, but the gullying process may begin to network again and increase the fractal dimension. This enunciates that the badlands are die-hard patterns of erosive processes that sculpt their form again in such lands which have been reclaimed by refilling and flattening the gullies. This is an important inference that can serve as a guideline to land

conservation designers in the badlands. It cautions that the same material of the locale should not be used as a fill for the gullies. The site S2 shows the general behaviour of the processes, which has increased in complexity as indicated in the successive increase of the fractal dimension. This represents such a case where no conservation plan was applied. The site S4 is a success story of such measures because it has been used for afforestation and soil material for refilling was brought from non-badland areas in the southwest.

The images taken for analysis for 2013 are of pre-monsoon time and D_q values for sites except S2 are less in comparison to 2003/2006 or 2018. The monsoonal precipitation for the year 2013 was considerably higher (Figure 8.4). Likewise, the result obtained from the Standard Precipitation Index (SPI) plot shows a water surplus year from 2011 to 2013 (Figure 8.5). Whereas, the rainfall distribution in 2003, 2006 and 2018 was near normal. The impact of rainfall may be taken into consideration as except S4, all the three sites show increase in D_q by 2018. It seems that heavy monsoonal rains of 2013 again triggered gullying at S1 and S3 sites defying the conservation measures taken prior to 2013 at these sites. There is a continuous decrease in the value of D_q in site S4, where conservation measures worked well throughout the observed years.

Thus, the variations of fractal dimension can be used as a criterion for determining and monitoring land conservation operation and it may also provide continuous feedback to improve the planning of such measures.

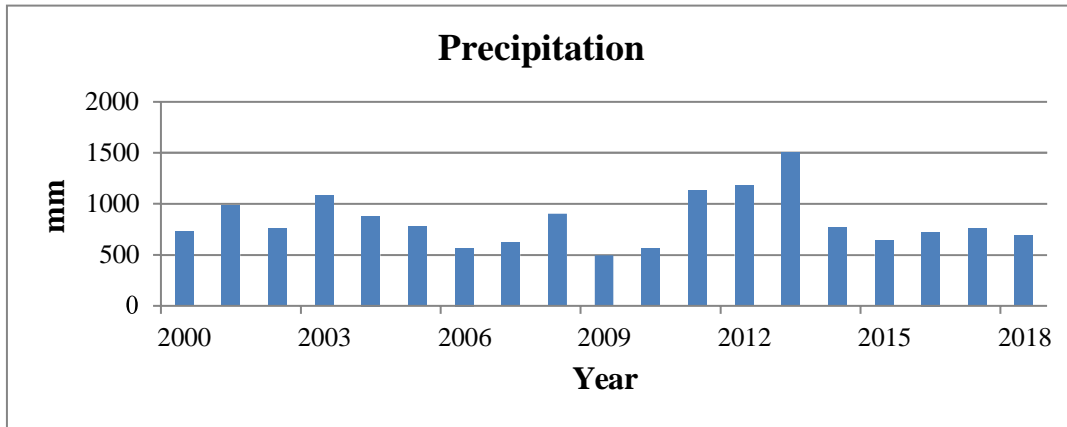


Figure 8. 4 Precipitation history from 2000 to 2018 of the study area (Source: India Meteorological Department)

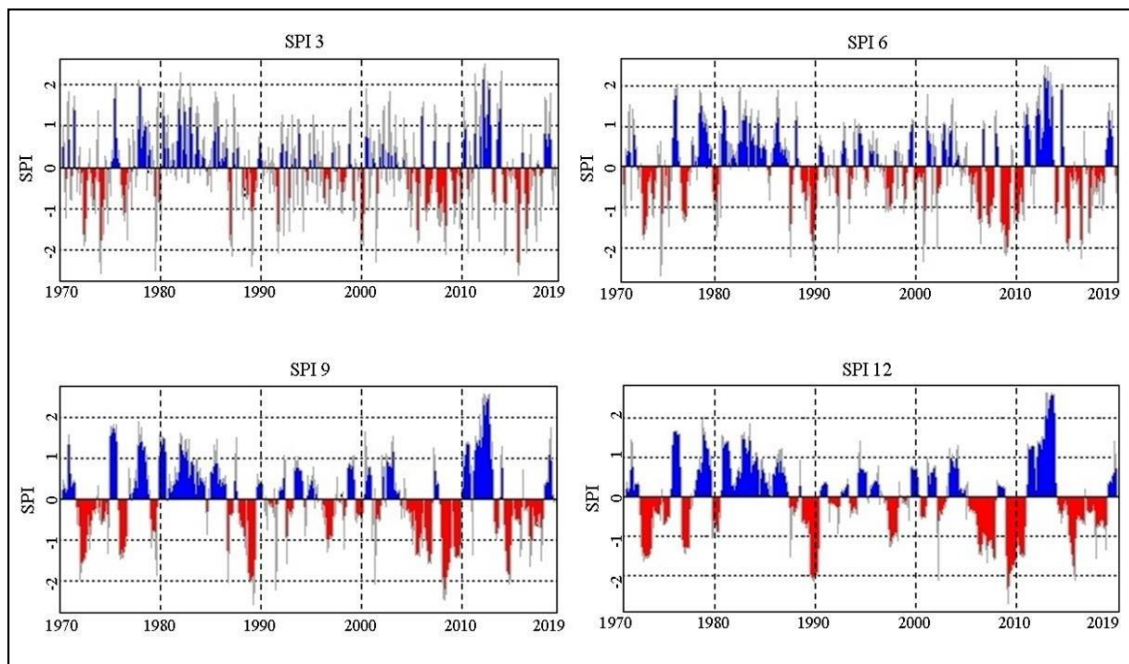


Figure 8. 5 Representation of SPI at different time scale of 3, 6, 9 and 12 months

The findings of Dq match well with the singularity component ($\Delta\alpha$) values which are also an important parameter in identifying the active change in form and relief through active erosion. It has been pointed out by earlier workers that the wider the probability distribution, the larger will be the elevation difference in the terrain. This shows a richer terrain profile in forms, which denotes active and dense gully erosion and fragmented surface (Cao et al., 2020). The ($\Delta\alpha$) value varies with fractal dimension (Dq) value in site S1, where the ($\Delta\alpha$) value decreases for the year 2013 but increases again in 2018. In site S2, these two parameters are almost similar with an extremely small increase for the observation period (Table 8.1), whereas S4 has experienced reclamation approaches. Because of these measures, Dq suddenly decreased around 2013; on the contrary, the $\Delta\alpha$ was found to be noticeably high for the same year, which is owing to an increase in α_{\max} value, possibly indicating the appearance of forms on the higher value of the exponent of scale. Later on, $\Delta\alpha$ value has further decreased in 2018, indicating adjustment of form with the general forms already existent. Site S4 is a vegetated site, has a decreasing trend of Dq . This type of form adjustment with general form is best seen in the S3 site, which shows a decrease in ($\Delta\alpha$) in 2018. A decrease in ($\Delta\alpha$) indicates an adjustment to dominant forms in the pattern.

The results of $f(\alpha)$ versus (α) further lend support to the observations made above in the discussion of fractal dimensions. The graph of $f(\alpha)$ versus (α) is typically hump-shaped for all the sites. The hump-shaped graphs show the multifractal nature of these gully link patterns of badlands. The peak value of $f(\alpha)$ is equal to the fractal dimension of the pattern. The graph of $f(\alpha)$ versus (α) exposes some implicate behaviour of the geomorphic process related to badlands formation. In the studied sites of the badlands, the graphs show shorter

left limbs and longer right limbs, presenting a right-skewed asymmetrical form of the curve. Oswiecimka et al. (2018) linked the right-side asymmetry in complex networks as a criterion to help assess the degree of complexity and even evaluate the clustering when it was difficult to determine. A right-skewed (positively skewed) graph represents such a dataset in which the mean value is always greater than median and mode values, implying that a greater number of the data has lower values than the mean value. The mean value of any system behaves rigidly; thereby, the lower values should tend to approach the mean value in a self-aggravating system. This implies that the system is increasing in complexity. This conclusion is well corroborated with the interpretation of $\Delta f(\alpha)$, as discussed below.

The asymmetry of the graph $f(\alpha)$ versus (α) provides an important parameter of the difference between the values of $f(\alpha)$ for the $(\alpha)_{\max}$ and $(\alpha)_{\min}$ of the graph denoted as $\Delta f(\alpha)$. If $\Delta f(\alpha)=0$ the dimension of the subset is equal with minimum value $f(\alpha)$, indicating that simple forms (tending to non-fractal form) exist at the maximum and minimum side of (α) ; hence the system is in equilibrium. However, if the graph is right-skewed and $\Delta f(\alpha)$ has a negative value, i.e., the $(\alpha)_{\max} < (\alpha)_{\min}$, indicating much complexity on the minimum side of (α) and implying rills are active. Should the graph be left-skewed (negatively skewed) in nature then, it would mean that the mean value is less than median and mode, indicating, most of the data is falling on the higher side of the mean. In such a case, the values would be pulled down towards the mean value and the system would be decreasing in complexity. When the graph is left-skewed and $\Delta f(\alpha)$ has a positive value, i.e. $(\alpha)_{\max} > (\alpha)_{\min}$, then it would mean levelling of the area towards the maximum value of the scale.

Thus, it is concluded that the present case is all the badlands of the area show $\Delta f(\alpha)$

values in negative values and are right-skewed, showing aggravating conditions of dissection patterns and self-enhancing phase of badlands formation. In other words, it can be said that the complexity is achieved by active erosion in the case of positively skewed fields, whereas processes of sedimentation and aggradation in the gullies are indicated in the negatively skewed graph. In the former case, the system should approach closer to the mono-fractal forms by densely dissecting the area, while in the latter case, the system shifts towards a non-fractal state by natural levelling of the area.

Very low values of lacunarity indicate the homogeneity of the pattern and reassure the multifractal nature of the gully- channel- badlands system (Table 8.1). The Lacunarity analysis also led to confirmation of results obtained by multifractal analysis in the present study.

Thus, the multifractal analytical approach can throw light on the implicate dynamism of the geomorphological processes and evolution of the involved system. On the basis of the results of the multifractal analysis, the badlands can be characterized by (a) patterns of gully systems which, after initiation, grow in the complexity of forms (b) the organization of patterns takes place through naturally selected branching of gully links towards upstream lands (c) the gully links are self-repetitive over space, (d) they form self-enhancing and ever-spreading systems in time until some boundary conditions.

8.5 Conclusions

The parameters of fractal analysis are found to be correlated with the geomorphological processes, their intensities and the complexity of the pattern generated. On the basis of the results and discussion, it can be concluded that the area is showing multifractal

characteristics. The lower value of lacunarity also confirms the same. Thus, the following conclusions can be drawn:

- I. The multifractal analysis is a strong tool to understand natural patterns like badlands. The badlands of the study area show high values of fractal dimension (D_q) with sigmoidal shaped decreasing towards higher values of Q ($Q > 0$) and low values of lacunarity (λ_g or Λ_g), indicating that the badlands are multifractally patterned and are densely dissected. Right skewed graphs and negative values of $\Delta f(\alpha)$ show that gullying processes are active on a finer scale through rill networking. The greater values ($\Delta\alpha$) show greater complexity in the study area and the decrease in ($\Delta\alpha$) may be indicative of adjustment of forms.
- II. The behavior of badlands forms a positive feedback loop of the self-enhancing type, which cannot be easily checked. The gully pattern quickly spreads and any changes in the complexity may be observed in a small duration of time.
- III. Once initial fractal patterns are generated, they keep on moving into the sound areas and quickly deteriorate their natural conditions. These patterns need to be taken care of with proper eco-friendly, locale-specific remedial measures. It may provide the basis for priority considerations for land conservation measures in the watershed affected by badlands conditions and soil losses.